Int. J. Open Problems Compt. Math., Vol. 11, No. 1, March 2018
ISSN 1998-6262;
www.i-csrs.org

Computing upper bound eigenvalues for Schrödinger operator

Eman Al kathiri

Department of Mathematics, College of Science and Arts,Najran University, Sharoura,
P.O.Box 19884 Kingdom Saudi Arabia.
e-mail:pinkflower201022@hotmail.com

Received 26 November 2017; Accepted 16 February 2018

Abstract

The objective of the present work is to compute the upper bound of the eigenvalues for one dimensional Schrödinger operator:

$$-u''(x) + V(x)u(x) = \lambda u(x)$$

We discuss two different methods: Galerkin method and Power method. We use finite element method as a technique to solve the problems. We consider two models: harmonic ($V(x) = x^P$: $P = 2$***) and anharmonic oscillators (*** $P = 6, 8$***). The piecewise, cubic Hermite and quintic elements have been used in our numerical results.Tables and figures exhibiting the main results are given.***

Keywords: *One dimensional Schrödinger operator; Cubic and quintic; Galerkin finite element method; Power method; Maple and Matlab programs.*
2017 Mathematics Subject Classification: *65M60, 65N30, 65N15.*

1 Introduction

In many branches of physical, engineering, biological, environmental, chemical, geophysical or medical sciences, most of the model problems simulating phenomena are three, two or one dimensional boundary value problems, which may be subject to certain initial conditions [2, 3, 4, 5, 6]. The problem reduces, in several cases of these boundary value problems, to the determination of the eigenfunctions and the corresponding eigenvalues of a certain differential operator.

An eigenfunction of a linear operator T defined on some function space is any non-zero function u in that space that, when acted upon by T, is only multiplied by some scaling factor. As an equation, this condition can be written as

$$Tu = \lambda u$$

where λ is a scalar in a field K, known as the eigenvalue, characteristic value, or characteristic root associated with the eigenfunction u.

The eigenvalues λ are generally limited to a discrete set $\lambda_1, \lambda_2, \cdots$ or to a continuous set over some range. The set of all possible eigenvalues of T is called its spectrum [2, 10, 14].

The most famous and important method adopted for computing the eigenvalues is the finite element method through which, an approximation technique for the solution of differential equations using piecewise polynomials is sought for [1, 11, 12, 15].
Many publications are devoted to the study of the finite element method in treating boundary value problems [9] and references included there in).
The main objective of the present work is to deal with the computation of the eigenfunctions and eigenvalues of the one dimensional Schrödinger operator subject to Dirichlet boundary conditions using finite element method.

We introduce the Galerkin finite element method for approximating the eigenvalues of differential operators, the spaces of the cubic Hermite basis functions and the quintic Hermite basis functions and present the power method, for the determination of the eigenvalues and eigenvectors of the square matrices.
We deal with the problem of the harmonic oscillator ($P = 2$). The problem is studied using the finite element method expressed in cubic and quintic Hermite finite elements. The study shows that the results obtained by the quintic Hermite finite elements are more accurate than those obtained by the cubic Hermite finite elements. A comparison study is carried out between the Galerkin method and the power method for the harmonic oscillator. It is shown that, the results obtained by the power method are almost the same as those of Galerkin method in the cubic case, while the results of the Galerkin method in the quintic case are strongly better than those of the power method.
We study the problem of anharmonic oscillator ($P = 6, 8$) using cubic and quintic Hermite finite elements. The study shows that the results obtained by the quintic Hermite finite elements are more accurate than those obtained by the cubic Hermite finite elements.
A conclusion of the work and the proposed future work and also two appendices containing important formulae are given.

2 Galerkin method

The Galerkin method is introduced in the work of Courant in the 1940s [2]. We would like to apply this method to one dimensional Schrödinger operator T acting on $L^2(\Omega)$. It is known that, in the finite element method, the subspaces $\mathcal{L}$, called finite element spaces, are constructed by assembling together polynomial functions defined on sub-domains of Ω. These sub-domains together with the polynomial functions are called elements. We will consider the cubic and quintic cases.
Let $L > 0$ and let $\Omega \subset \mathbb{R}$ be an open bounded set $\Omega = [-L, L]$ and let $V : \Omega \to \mathbb{R}$ be a continuous function. Shrödinger operator T with potential $V(x)$ in the region Ω is defined as

$$Tu(x) = -u''(x) + V(x)u(x) \qquad , x \in \Omega. \tag{1}$$

This is a self-adjoint operator acting on $L^2(\Omega)$ and subject to Dirichlet boundary conditions:

$$u(-L) = u(L) = 0. \tag{2}$$

In the present work the potentials $V(x)$ will be considered as

$$V(x) = x^P, \quad P = 2, 6, 8. \tag{3}$$

We note that these potentials are bounded from below and it can be shown that this Shrödinger operator is a self-adjoint operator on Hilbert space $\mathcal{H}$ with real eigenvalues. To use Galerkin finite element method for the determination of the eigenvalues of Schrödinger operator, we carry out the following processes.

1. Derive a weak formulation in integral form of the problem. This can be done by multiplying a test function $v(x)$, with $v(-L) = v(L) = 0$ to both sides of the eigenvalue problem:

   $$(-u'' + V(x)u)v = (\lambda u)v \tag{4}$$

   Integrating from $-L$ to L, we get after some calculations

   $$\int_{-L}^{L} u'v'dx + \int_{-L}^{L} (V(x)uv)dx = \lambda \int_{-L}^{L} (uv)dx. \tag{5}$$

   This form is called the weak form of Shrödinger operator.

2. Generate mesh (interval). For example, we use a uniform Cartesian mesh
   $x_i = -L + ih$.
   $i = 0, 1, \cdots, n$.
   $h = \frac{2L}{n}$.
   to get the sub-intervals $[x_{i-1}, x_i], i = 1, 2, \cdots, n$. This means division the interval into n sub-intervals with end points at

   $$-L = x_0 < x_1 < \cdots < x_{n-1} < x_n = L.$$

3. Construct a set of basis functions $\phi_j(x), j = 1, 2, \cdots, n-1$.consisting of piecewise continuous functions (cubic or quintic) in each sub-interval vanishing at $-L$ and L.

4. We put the approximate solution as a linear combination of the basis functions in the form:

$$u_h(x) = \sum_{i=1}^{n-1} \alpha_i \phi_i(x). \tag{6}$$

where the coefficients α_i are *unknowns.* The function $u_h(x)$ is a piecewise basis function, and is not the exact solution. Using the weak form and denoting

   a. The stiffness matrix

$$A : a_{ij} = \int_{-L}^{L} \phi_i{}' \phi_j{}' dx. \tag{7}$$

   b. The mass matrix

$$B : b_{ij} = \int_{-L}^{L} \phi_i \phi_j dx. \tag{8}$$

   c. The bending matrix

$$C : c_{ij} = \int_{-L}^{L} V(x) \phi_i \phi_j dx. \tag{9}$$

we get the linear system of equations

$$D\alpha = \lambda\alpha. \tag{10}$$

where $[\alpha]$ is the eigenvector corresponding to the generalized eigenvalue and

$$D = \left(B^{-1}\right)(A + C). \tag{11}$$

5. Find the generalized eigenvalues. Using one of the famous methods (Power method, Inverse power method and Command 'eigs' in Matlab ...etc).

2.1 Cubic basis functions

In this case of cubic basis functions the space $\mathcal{L}$ is generated by piecewise continuous functions cubic in each sub-interval vanishing at $-L$ and L. These are Hermite elements of order $r = 3$ forming a basis of $\mathcal{L}$. The associated basis

functions $P_i(x)$ and $Q_i(x)$ over two contiguous segments in the mesh are given in appendix A.
The set of basis functions $\phi_i(x), i = 1, 2, \cdots, N.$ with $N = (2n-2)$ is given by

$$\phi_{2i-1}(x) = P_i(x), \quad \phi_{2i}(x) = Q_i(x), \tag{12}$$

where $i = 1, \cdots, (n-1)$, $h = \frac{2L}{n}$, $-L = x_0$ and $x_n = L$.
In this case the stiffiness matrix $\mathbf{A}$ and the mass matrix $\mathbf{B}$ are defined as:

$$\mathbf{A} = \left[\langle \phi_i', \phi_j' \rangle\right]_{i,j=1}^{2\cdot(n-1)}, \quad \mathbf{B} = \left[\langle \phi_i, \phi_j \rangle\right]_{i,j=1}^{2\cdot(n-1)}. \tag{13}$$

The approximate solution 6 takes the form

$$u_h(x) = \sum_{i=1}^{N} \alpha_i \phi_i(x). \tag{14}$$

2.2 Quintic basis functions

The space $\mathcal{L}$ is generated by piecewise continuous functions quintic in each sub-interval vanishing at $-L$ and L. These are Hermite elements of order $r = 5$ forming a basis of $\mathcal{L}$. The associated basis functions $P_i(x)$, $Q_i(x)$ and $R_i(x)$ over two contiguous segments in the mesh are in given appendix B.
The set of basis functions $\phi_i(x), i = 1, 2, \cdots, N.$ with $N = (3n-3)$ is given by

$$\phi_{3i-2}(x) = P_i(x), \quad \phi_{3i-1}(x) = Q_i(x), \quad \phi_{3i}(x) = R_i(x), \tag{15}$$

where $i = 1, \cdots, (n-1)$, $h = \frac{2L}{n}$, $-L = x_0$ and $x_n = L$.
In this case, the stiffiness matrix $\mathbf{A}$ and the mass matrix $\mathbf{B}$ take the form

$$\mathbf{A} = \left[\langle \phi_i', \phi_j' \rangle\right]_{i,j=1}^{3\cdot(n-1)}, \quad \mathbf{B} = \left[\langle \phi_i, \phi_j \rangle\right]_{i,j=1}^{3\cdot(n-1)}. \tag{16}$$

The approximate solution $u_h(x)$ is similar to 14 with $N = (3n-3)$.

3 Examples

3.1 The harmonic oscillator with potential $V(x) = x^2$

The harmonic oscillator is the case for which $P = 2$. Schrödinger operator in this case has exact eigenvalues $\lambda_i = 1, 3, 5, 7, 9, \cdots$. Applying the above mentioned procedure for the approximate calculation of the eigenvalues, the results tabulated in the following tables are obtained.

i	λ_i (Exact)	λ_i (Approximate)	Absolute error
1	1.000000000000000	1.000000000000291	2.911×10^{-13}
2	3.000000000000000	3.000000000002690	2.691×10^{-12}
3	5.000000000000000	5.000000000012188	1.219×10^{-11}
4	7.000000000000000	7.000000000038342	3.834×10^{-11}
5	9.000000000000000	9.000000000095254	9.525×10^{-11}

Table 1: The first five eigenvalues of T^{har} calculated using cubic Hermite elements with $n = 600$ (i.e. $h \approx 0.03$) in the domain $\Omega = [-10, 10]$.

i	λ_i (Exact)	λ_i (Approximate)	Absolute error
1	1.000000000000000	1.000000000000003	2.665×10^{-15}
2	3.000000000000000	3.000000000000013	1.288×10^{-14}
3	5.000000000000000	5.000000000000008	7.994×10^{-15}
4	7.000000000000000	6.999999999999995	5.329×10^{-15}
5	9.000000000000000	8.999999999999993	7.105×10^{-15}

Table 2: The first five eigenvalues of T^{har} calculated using quintic Hermite elements with $n = 200$ (i.e. $h = 0.1$) in the domain $\Omega = [-10, 10]$.

A simple comparison between the results tabulated in tables 1, 2 show that the quintic Hermite elements method with $n = 200$ (i.e. $h = 0.1$) gives more accurate and superior results than the method of cubic Hermite elements.
In Figure 1, we show loglog pictures of $\frac{1}{n}$ in the horizontal axis and the absolute error $|\lambda_{approx} - \lambda_{exact}|$ in the vertical axis. As calculated using cubic Hermite elements in the domain $\Omega = [-10, 10]$, the slopes of the graphs are close to the value 6.

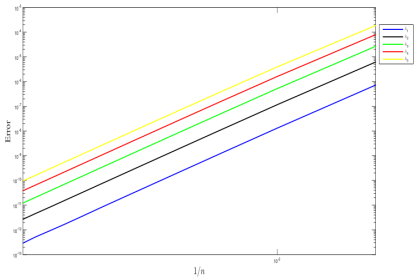

Figure 1: Loglog plot for the first five approximate eigenvalues of T^{har}. The slopes are all close to the value 6 by cubic Hermite elements. The horizontal axis is $\frac{1}{n}$ and the vertical axis is absolute error $|\lambda_{approx} - \lambda_{exact}|$.

In Figure 2, we show loglog pictures of $\frac{1}{n}$ in the horizontal axis and the absolute error $|\lambda_{approx} - \lambda_{exact}|$ in the vertical axis. As calculated using quintic

Hermite elements in the domain $\Omega = [-10, 10]$, the slopes of the graphs are close to the value 11.

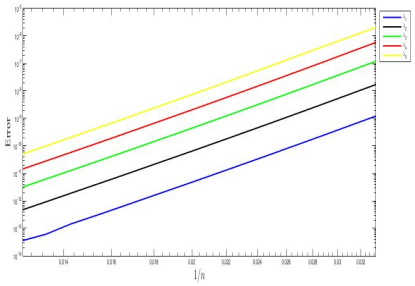

Figure 2: Loglog plot for the first five approximate eigenvalues of T^{har}. The slopes are all close to the value 11 by quintic. The horizontal axis is $\frac{1}{n}$ and the vertical axis is absolute error $|\lambda_{approx} - \lambda_{exact}|$.

To compute the slopes of the straight lines appearing in figures 1, 2 we used the command "polyfit" implemented in Matlab.
We are not aware of any publication that takes into consideration the approximation of the eigenvalues of T^{har} using the quintic Hermait elements method which we obtained in this subsection.
Hobiny (2014), [9] treated the same case of harmonic oscillator using cubic Hermite elements with $n = 400$ (i.e. $h = 0.03$) in the domain $\Omega = [-6, 6]$. The error which he obtained for the first eigenvalue was of the order of 10^{-13} and the error for the fifth eigenvalue was of the order of 10^{-9}. Our results seem to be more accurate.

3.2 The anharmonic oscillator

The anharmonic oscillator is the case for which $P \neq 2$. Schrödinger operator in this case has not known exact eigenvalues. We consider two cases of the anharmonic oscillator, precisely the cases $P = 6, 8$.

3.2.1 The anharmonic oscillator with potential $V(x) = x^6$

Applying the above mentioned procedure for the approximate calculation of the eigenvalues, the results tabulated in the following tables are obtained.

i	λ_i (quintic)	λ_i (cubic)	Absolute difference
1	1.144802453797060	1.144802453802710	5.649×10^{-12}
2	4.338598711514002	4.338598711573214	5.921×10^{-11}
3	9.073084560921512	9.073084561349365	4.279×10^{-10}
4	14.935169634911382	14.935169637064174	2.153×10^{-9}
5	21.714165422200331	21.714165430268860	8.069×10^{-9}

Table 3: Approximate eigenvalues for T^{anh} with $P = 6$ with $n = 600$ using cubic Hermite elements.

From table 3 we show that the difference between the eigenvalue λ_1 calculated from the quintic and the cubic cases is of the order of 10^{-12} and increases gradually with the increase of the eigenvalue. Considering the results obtained by quintic Galerkin finite element method for $n = 200$ (i.e. $h = 0.1$) as exact eigenvalues, figure 3 gives the log log plot of $\frac{1}{n}$ in the horizontal axis and the absolute error $|\lambda_{quintic} - \lambda_{cubic}|$ in the vertical axis, as calculated using cubic Hermite elements in the domain $\Omega = [-10, 10]$, the slopes of the graphs are close to the value 6.

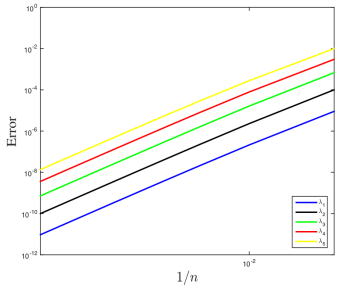

Figure 3: Loglog plot for the first five approximate eigenvalues of T^{anh} with $P = 6$. The slopes are all close to the value 6 by piecewise cubic Hermite elements. The horizontal axis is $\frac{1}{n}$ and the vertical axis is the absolute error $|\lambda_{approx} - \lambda_{exact}|$.

Figure 4 gives the log log plot of $\frac{1}{n}$ in the horizontal axis and the absolute error $|\lambda_{approx} - \lambda_{exact}|$ in the vertical axis, as calculated using quintic Hermite elements in the domain $\Omega = [-10, 10]$, the slopes of the graphs are close to the value 11.

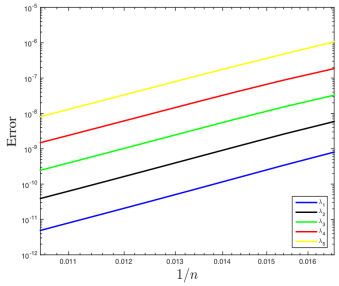

Figure 4: Loglog plot for the first five approximate eigenvalues of T^{anh} with $P = 6$. The slopes are all close to the value 11 by quintic Hermite elements. The horizontal axis is $\frac{1}{n}$ and the vertical axis is the absolute error $|\lambda_{approx} - \lambda_{exact}|$.

3.2.2 The anharmonic oscillator with potential $V(x) = x^8$

Applying the above mentioned procedure for the approximate calculation of the eigenvalues, the results tabulated in the following tables are obtained.

i	λ_i (quintic)	λ_i (cubic)	Absolute difference
1	1.225820113800515	1.225820113821599	2.108×10^{-11}
2	4.755874413960940	4.755874414128003	1.671×10^{-10}
3	10.244946977237715	10.244946978267270	1.029×10^{-9}
4	17.343087970589508	17.343087975673772	5.084×10^{-9}
5	25.809006751314829	25.809006771000966	1.969×10^{-8}

Table 4: Approximate eigenvalues for T^{anh} with $P = 8$ with $n = 600$ using cubic Hermite elements.

From table 4 we show that the difference between the eigenvalue λ_1 calculated from the quintic and the cubic cases is of the order of 10^{-11} and increases gradually with the increase of the eigenvalue.
Considering the results obtained by Galerkin quintic finite element method for $n = 200$ (i.e. $h = 0.1$) as exact eigenvalues, figure 5 gives the log log plot of $\frac{1}{n}$ in the horizontal axis and the absolute error $|\lambda_{quintic} - \lambda_{cubic}|$ in the vertical axis, as calculated using cubic Hermite elements in the domain $\Omega = [-10, 10]$, the slopes of the graphs are close to the value 6.

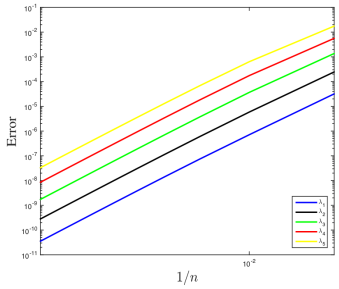

Figure 5: Loglog plot for the first five approximate eigenvalues of T^{anh} with $P = 8$. The slopes are all close to the value 6 by cubic Hermite elements. The horizontal axis is $\frac{1}{n}$ and the vertical axis is the absolute error $|\lambda_{approx} - \lambda_{exact}|$.

Figures 6 gives the log log plot of $\frac{1}{n}$ in the horizontal axis and the absolute error $|\lambda_{approx} - \lambda_{exact}|$ in the vertical axis, as calculated using quintic Hermite elements in the domain $\Omega = [-10, 10]$, the slopes of the graphs are close to the value 12.

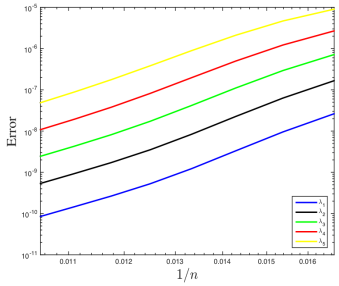

Figure 6: Loglog plot for the first five approximate eigenvalues of T^{anh} with $P = 8$. The slopes are all close to the value 12 by quintic Hermite elements. The horizontal axis is $\frac{1}{n}$ and the vertical axis is the absolute error $|\lambda_{approx} - \lambda_{exact}|$.

The accuracy of the calculated eigenvalues is so high that we can consider these values as the exact eigenvalues and we will use them in the comparison process with the results obtained by other methods.

4 Power method

In the above tables, we used the command 'eigs' implemented in Matlab to calculate the eigenvalues of matrices. We are aware of many other methods devoted for the calculation of both eigenvalues and eigenvectors of matrices such as the **Power method** [7, 8, 13]
In the present section we carry out a comparison study between the results

obtained by applying the Galerkin method and the power method for the case of harmonic oscillator T^{har}. This study will consider the cases of cubic and quintic basis functions. The comparison is exhibited in the following tables:

i	λ_i(Exact)	λ_i by power method	Absolute error	λ_i by cubic Galerkin method	Absolute error
1	1	1.000000000000276	2.760×10^{-13}	1.000000000000291	2.911×10^{-13}
2	3	3.000000000002682	2.682×10^{-12}	3.000000000002690	2.691×10^{-12}
3	5	5.000000000012037	1.204×10^{-11}	5.000000000012188	1.219×10^{-11}
4	7	7.000000000038405	3.840×10^{-11}	7.000000000038342	3.834×10^{-11}
5	9	9.000000000095170	9.517×10^{-11}	9.000000000095254	9.525×10^{-11}

Table 5: Comparison between the power method and the Galerkin method in the cubic Hermite elements case for the first five eigenvalues of T^{har}.

i	λ_i(Exact)	λ_i by power method	Absolute error	λ_i by quintic Galerkin method	Absolute error
1	1	0.999999999989234	1.077×10^{-11}	1.000000000000003	2.665×10^{-15}
2	3	2.999999999994227	5.773×10^{-12}	3.000000000000013	1.288×10^{-14}
3	5	4.999999999975480	2.452×10^{-11}	5.000000000000008	7.994×10^{-15}
4	7	6.999999999982064	1.794×10^{-11}	6.999999999999995	5.329×10^{-15}
5	9	8.999999999976112	2.389×10^{-11}	8.999999999999993	7.105×10^{-15}

Table 6: Comparison between the power method and the Galerkin method in the quintic Hermite elements case for the first five eigenvalues of T^{har}.

The above tables show that the results obtained by the power method are almost the same as those of Galerkin method in the cubic case, while the results of the Galerkin method are strongly better than those of the power method. Based on the results in the above tables, we obtain the following figures clarifying the behavior of the error in the cubic and the quintic cases.

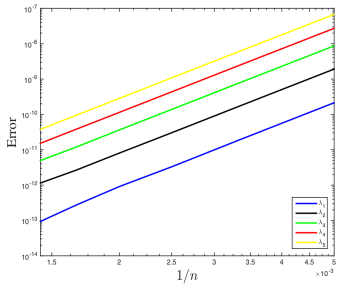

Figure 7: Loglog plot for the first five approximate eigenvalues of T^{har} with power method. The slopes are all close to the value 6 by cubic Hermite elements. The horizontal axis is $\frac{1}{n}$ and the vertical axis is absolute error $|\lambda_{approx} - \lambda_{exact}|$.

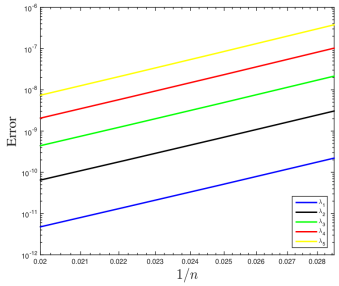

Figure 8: Loglog plot for the first five approximate eigenvalues of T^{har} with power method. The slopes are all close to the value 11 by quintic Hermite elements. The horizontal axis is $\frac{1}{n}$ and the vertical axis is absolute error $|\lambda_{approx} - \lambda_{exact}|$.

The slopes of the straight lines shown in these figures for the cubic and quintic cases are 6 and 11 respectively.
These results and behavior of the error go in agreement with theorem 6.1 in [15] which states that " The error in the approximation of the eigenvalues of a one dimensional elliptic problem of order k by using Hermite elements of order p is proportional to $h^{2(p+1-k)}$ ".
We carried out the same comparison procedure in the cases of anharmonic oscillator (P=6,8) using quintic bases functions, and the results of the application of the power method and the Galerkin method have been shown to be very closed to each other.

5 Discussion

We limit ourselves to the harmonic case (P=2). We carried out the procedure explained above for different values of n using quintic bases functions. We obtained the following results:

i	Error for $n = 15$	Error for $n = 20$	Error for $n = 40$	Error for $n = 60$	Error for $n = 80$
1	4.062×10^{-6}	5.525×10^{-8}	5.185×10^{-11}	7.092×10^{-13}	3.664×10^{-14}
2	4.194×10^{-6}	2.516×10^{-6}	7.122×10^{-10}	9.508×10^{-12}	4.872×10^{-13}
3	2.275×10^{-4}	1.151×10^{-6}	4.946×10^{-9}	6.424×10^{-11}	3.222×10^{-12}
4	3.694×10^{-4}	8.691×10^{-5}	2.339×10^{-8}	2.953×10^{-10}	1.460×10^{-11}
5	1.647×10^{-3}	1.032×10^{-5}	8.541×10^{-8}	1.049×10^{-9}	5.114×10^{-11}

Table 7: Absolute errors for values of n between 15 and 80.

i	Error for $n = 100$	Error for $n = 200$	Error for $n = 300$	Error for $n = 400$	Error for $n = 500$
1	6.661×10^{-16}	2.665×10^{-15}	1.776×10^{-15}	5.174×10^{-14}	1.310×10^{-14}
2	7.149×10^{-14}	1.288×10^{-14}	1.155×10^{-14}	6.262×10^{-14}	7.327×10^{-14}
3	3.109×10^{-13}	7.994×10^{-15}	2.842×10^{-14}	1.110×10^{-13}	7.994×10^{-14}
4	1.502×10^{-12}	5.329×10^{-15}	4.529×10^{-14}	1.190×10^{-13}	1.235×10^{-13}
5	5.0928×10^{-12}	7.105×10^{-15}	1.599×10^{-14}	1.101×10^{-13}	2.895×10^{-13}

Table 8: Absolute errors for values of n between 100 and 500.

i	Error for $n = 600$	Error for $n = 700$	Error for $n = 800$	Error for $n = 900$	Error for $n = 1000$
1	3.642×10^{-14}	1.332×10^{-14}	3.078×10^{-13}	2.975×10^{-14}	1.739×10^{-13}
2	1.332×10^{-15}	6.573×10^{-14}	1.181×10^{-13}	7.860×10^{-14}	4.769×10^{-13}
3	1.155×10^{-14}	8.438×10^{-14}	3.615×10^{-13}	9.859×10^{-14}	4.761×10^{-13}
4	1.776×10^{-14}	8.971×10^{-14}	3.233×10^{-13}	2.043×10^{-14}	5.542×10^{-13}
5	4.086×10^{-14}	6.750×10^{-14}	8.419×10^{-13}	1.847×10^{-13}	7.283×10^{-13}

Table 9: Absolute errors for values of n between 600 and 1000.

The above tables show that the best result was obtained for $n = 200$ (i.e. $h = 0.1$). However it was expected that the error decreases as n increases but here we see that for $n > 200$ the error increases irregularly with the increase of n.
The reason of this unexpected result in our point of view may be the following: The error tabulated in the above tables is the total error and this includes the error of the method and the usual numerical errors, namely the rounding, the truncation and the accumulation errors.
The accumulation error increases with the increase of the number of computation steps and these steps increase hugely with the increase of n in such a way that the accumulation error deteriorates the improvement of the accuracy taking place with the increase of n.
Tables, 1 and 7 show that the results obtained in the quintic case for $n = 80$ (i.e. $h = 0.25$) are more accurate than those for the cubic case for $n = 600$ (i.e. $h \approx 0.03$).
These remarks assert the powerful and necessity of the Galerkin quintic finite element method in studying the harmonic oscillator T^{har}.

6 Open Problems

As open problems, we propose the following items:

(1) Studying whether or not using Hermite finite elements of orders higher than the fifth order can improve the accuracy of the Galerkin method used for the solution.

(2) Studying similar problems with different types of boundary conditions such as Neuman, Robin or mixed boundary conditions.

(3) Generalizing the work included in this paper to cover the cases of two and three dimensional problems.

(4) Using the explained procedure to study other problems of interest in other domains of physical sciences such as thermodynamics, fluid mechanics, elasticity, etc.

(5) Trying to study the solution of some sorts of nonlinear operators using the Galerkin finite element method along with an iteration technique.

References

[1] P. Arbenz, *Finite element interpolation error bounds with applications to eigenvalue problems*, Zeitschrift fur Angewandte Mathematik und Physik (ZAMP), 34.2, (1983), 180-191.

[2] L. Boulton and M. Levitin, *Trends and Tricks in Spectral Theory,* Ediciones IVIC, (2007).

[3] L. Boulton and M. Levitin, *On approximation of the eigenvalues of perturbed periodic Schroedinger operators*, Journal of Physics. A, Mathematical and Theoretical (Online), 40.31, (2007), 9319-9329.

[4] L. Boulton, N. Boussaid, and M. Lewin, *Generalized Weyl theorems and spectral pollution in the Galerkin method*, Journal of Spectral Theory, 2.4, 329-354, (2012).

[5] L. Boulton and A. Hobiny, *On the convergence of the quadratic method*, IMA Journal of Numerical Analysis, 36.3, (2015), 1310-1333.

[6] L. Boulton and A. Hobiny, *On the quality of complementary bounds for eigenvalues*, Calcolo, 52.4, (2015), 577-601

[7] R. Butt, *Introduction to Numerical Analysis Using MATLAB*, Jones and Bartlett Learning, (2009).

[8] H. Golub and F. Van Loan, *Matrix computations*, Vol. 3. JHU Press, (2012).

[9] A. Hobiny, *Enclosures for the eigenvalues of self-adjoint operators and applications to Schrodinger operators*, Diss. Heriot-Watt University, (2014).

[10] E. Kreyszig, *Introductory functional analysis with applications,* Vol. 1. New York: wiley, (1989).

[11] Y. W. Kwon and H. Bang, *The finite element method using MATLAB,* CRC press, (2014).

[12] Z. Qiao, Z. Li, and T. Tang, *Numerical Solution of Differential Equations: Introduction to Finite Difference and Finite Element Methods*, Cambridge University Press, (2017).

[13] A. Quarteroni, R. Sacco and F. Saleri, *Numerical mathematics.* (Texts in applied mathematics; 37), New York: Springer-Verlag, (2002).

[14] B. P. Rynne, and M. A. Youngson, *Linear functional analysis*, Springer Science and Business Media, 2008.

[15] G. Strang and G. J. Fix, *An analysis of the finite element method*, Vol. 212. Englewood Cliffs, NJ:Prenticehall, (1973).

[16] H. Vosoughi and S. Abbasbandy, *Cardinal Basis Piecewise Hermite Interpolation on Fuzzy. Data*, Advances in Fuzzy Systems (2016).

Appendices

A Formulae for cubic case.

In the cubic case, the basis functions $P_i(x)$ and $Q_i(x)$ over two contiguous segments in the mesh are given by:

$$P_i(x) = \begin{cases} \frac{-(x-x_{i-1})^2(x_{i-1}-3x_i+2x)}{(x_i-x_{i-1})^3} & x_{i-1} \leqslant x \leqslant x_i, \\ \frac{(x-x_{i+1})^2(x_{i+1}-3x_i+2x)}{(x_{i+1}-x_i)^3} & x_i \leqslant x \leqslant x_{i+1}, \\ 0 & otherwise, \end{cases}$$

$$Q_i(x) = \begin{cases} \frac{(x-x_i)(x-x_{i-1})^2}{(x_i-x_{i-1})^2} & x_{i-1} \leqslant x \leqslant x_i, \\ \frac{(x-x_i)(x-x_{i+1})^2}{(x_{i+1}-x_i)^2} & x_i \leqslant x \leqslant x_{i+1}, \\ 0 & otherwise, \end{cases}$$

where $i = 1, \cdots, (n-1)$, $h = \frac{2L}{n}$, $-L = x_0$ and $x_n = L$.
A plot of each basis function is given in Figure A.1.

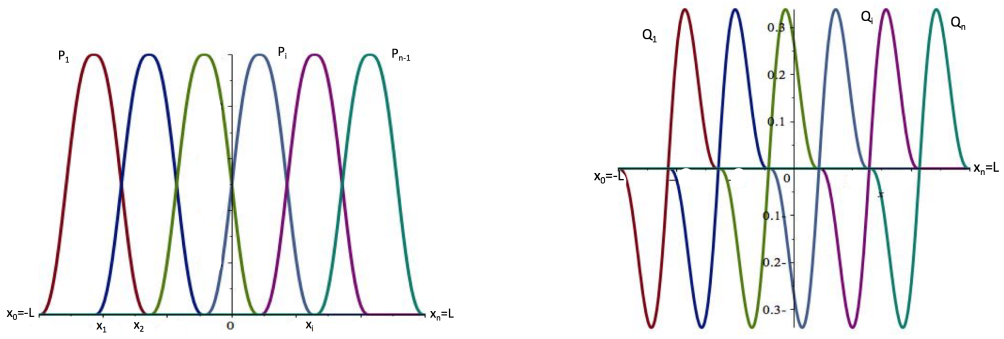

(a) $P_i(x)$ (b) $Q_i(x)$

Figure A.1: Cubic Hermite basis functions.

B Formulae for quintic case.

In the quintic case, the basis functions $P_i(x)$, $Q_i(x)$ and $R_i(x)$ given by [16]:

$$P_i(x) = \begin{cases} \frac{(x_{i-1}-x)^3}{(x_i-x_{i-1})^5}[(x_{i-1}+3x)(x_{i-1}-5x_i)+6x^2+10x_i^2], & x_{i-1} \le x \le x_i, \\ \frac{(x_{i+1}-x)^3}{(x_{i+1}-x_i)^5}[(x_{i+1}+3x)(x_{i+1}-5x_i)+6x^2+10x_i^2], & x_i \le x \le x_{i+1}, \\ 0 & otherwise, \end{cases}$$

$$Q_i(x) = \begin{cases} (\frac{x_{i-1}-x}{x_{i-1}-x_i})^3(x-x_i)[1+3\frac{x-x_i}{x_{i-1}-x_i}], & x_{i-1} \le x \le x_i, \\ (\frac{x_{i+1}-x}{x_i-x_{i+1}})^3(x_i-x)[1+3\frac{x_i-x}{x_i-x_{i+1}}], & x_{i-1} \le x \le x_i, \\ 0 & otherwise, \end{cases}$$

$$R_i(x) = \begin{cases} (\frac{x_{i-1}-x}{x_{i-1}-x_i})^3 \ \frac{(x_i-x)^2}{2}, & x_{i-1} \le x \le x_i, \\ (\frac{x-x_{i+1}}{x_i-x_{i-1}})^3 \ \frac{(x_i-x)^2}{2}, & x_{i-1} \le x \le x_i, \\ 0 & otherwise, \end{cases}$$

where $i = 1, \cdots, (n-1)$, $h = \frac{2L}{n}$, $-L = x_0$ and $x_n = L$.

A plot of each basis function is given in Figure B.1.

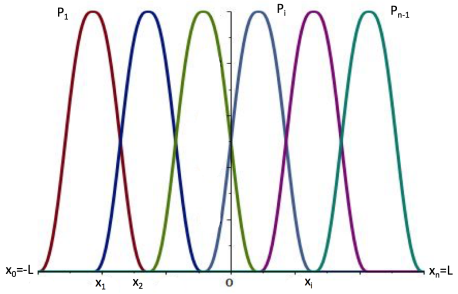

(a) $P_i(x)$

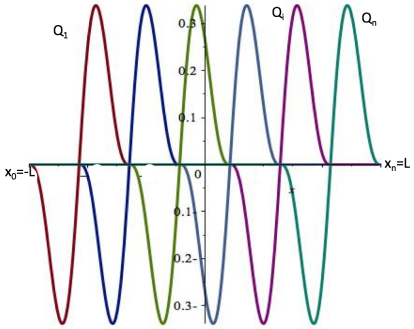

(b) $Q_i(x)$

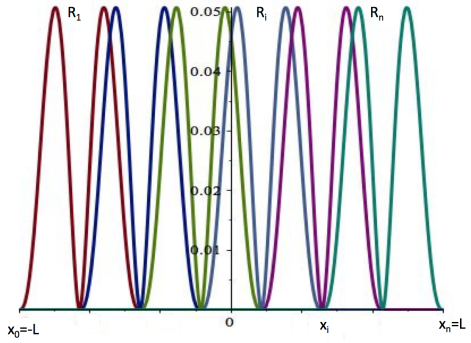

(c) $R_i(x)$

Figure B.1: Quintic Basis functions.